Measurement of the $D^{*\pm}$ cross section in two-photon processes

R. Enomoto,[1] M. Iwasaki,[2] K. Muramatsu,[2] H. Hayashii,[2] A. Miyamoto,[1] R. Itoh,[1] K. Abe,[3] T. Abe,[4] I. Adachi,[1]
M. Aoki,[4] S. Awa,[2] R. Belusevic,[1] K. Emi,[3] H. Fujii,[1] K. Fujii,[1] T. Fujii,[5] J. Fujimoto,[1] K. Fujita,[6] N. Fujiwara,[2]
B. Howell,[7] N. Iida,[1] H. Ikeda,[1] H. Iwasaki,[1] R. Kajikawa,[4] S. Kato,[8] S. Kawabata,[1] H. Kichimi,[1] M. Kobayashi,[1]
D. Koltick,[7] I. Levine,[7] K. Miyabayashi,[4] K. Nagai,[9] T. Nagira,[2] E. Nakano,[4] K. Nakabayashi,[4] O. Nitoh,[3]
S. Noguchi,[2] F. Ochiai,[10] Y. Ohnishi,[4] H. Okuno,[8] T. Okusawa,[6] K. Shimozawa,[4] T. Shinohara,[3] A. Sugiyama,[4]
N. Sugiyama,[11] S. Suzuki,[4] K. Takahashi,[3] T. Takahashi,[6] M. Takemoto,[2] T. Tanimori,[11] T. Tauchi,[1] F. Teramae,[4]
Y. Teramoto,[6] N. Toomi,[2] T. Toyama,[4] T. Tsukamoto,[1] S. Uno,[1] Y. Watanabe,[11] A. Yamaguchi,[2]
A. Yamamoto,[1] and M. Yamauchi[1]

[1] National Laboratory for High Energy Physics, KEK, Ibaraki-ken 305, Japan
[2] Department of Physics, Nara Women's University, Nara 630, Japan
[3] Department of Applied Physics, Tokyo University of Agriculture and Technology, Tokyo 184, Japan
[4] Department of Physics, Nagoya University, Nagoya 464, Japan
[5] Department of Physics, University of Tokyo, Tokyo 113, Japan
[6] Department of Physics, Osaka City University, Osaka 558, Japan
[7] Department of Physics, Purdue University, West Lafayette, Indiana 47907
[8] Institute for Nuclear Study, University of Tokyo, Tokyo 188, Japan
[9] The Graduate School of Science and Technology, Kobe University, Kobe 657, Japan
[10] Faculty of Liberal Arts, Tezukayama Gakuin University, Nara 631, Japan
[11] Department of Physics, Tokyo Institute of Technology, Tokyo 152, Japan

We have measured the inclusive $D^{*\pm}$ production cross section in a two-photon collision at the KEK e^+e^- collider TRISTAN. The mean $\sqrt{s}$ of the collider was 57.16 GeV and the integrated luminosity was 150 pb^{-1}. The differential cross section $[d\sigma(D^{*\pm})/dP_T]$ was obtained in the P_T range between 1.6 and 6.6 GeV and compared with theoretical predictions, such as those involving direct and resolved photon processes.

Hadron production in two-photon collisions is described by the vector-meson dominance model, the quark-parton model (direct process) [1], and the hard scattering of the hadronic constituents of almost-real photons (resolved photon process) [2–5], which has been observed by previous experiments [6]. However, more detailed studies are necessary in order to understand these processes quantitatively. Heavy quark pair production processes are good probes, since the theoretical calculations are less ambiguous than for light quarks [7].

The previous measurements had been carried out at around $\sqrt{s} \simeq 30$ GeV [8–10], and are consistent with a recent theoretical prediction [7]. At the energy of the KEK e^+e^- collider TRISTAN ($\sqrt{s} \simeq 60$ GeV), the $c\bar{c}$ production cross section becomes sizable; we have obtained the largest statistics for this type of process. We carried out a measurement of the $D^{*\pm}$ production cross section at a P_T greater than 1.6 GeV in two-photon collision events.

Details of the TOPAZ detector can be found elsewhere [11]. The integrated luminosity of the event sample used in the analysis was 150 pb^{-1}. The mean $\langle \sqrt{s} \rangle$ of the collider was 57.16 GeV. The trigger conditions are as follows: more than two tracks with $P_T > 0.3 \sim 0.7$ GeV and opening angle $> 45\sim70$ degrees (depending on the beam condition); a neutral energy deposit in the barrel calorimeter greater than 4 GeV; or that in the endcap calorimeters greater than 10 GeV.

The selection criteria for two-photon events are as follows: number of charged tracks ≥ 4; total visible energy in the central part of the detector between 4 and 25 GeV; vector sum of the transverse momenta of the particles with respect to the beam axis ($|\sum \mathbf{P}_T|$) less than 7.5 GeV; sum of the charges ≤ 3; event vertex consistent with the beam crossing point; and no large energy clusters ($E > 0.25 E_{\text{beam}}$) in the barrel calorimeter. In addition, we divided each event into two jets with respect to the plane perpendicular to the thrust axis, and the cosine of the angle between the two jets was required to be greater than -0.9. These restrictions were made in order to reduce beam gas, and single-photon-exchange events. A total of 10788 events was selected.

The charged track selections were as follows: closest approach to the event vertex consistent within the measurement error; the number of degrees of freedom (N_{df}) in the track fitting ≥ 3; and $P_T \geq 0.15$ GeV.

The γ selections were: cluster detected by a barrel-type lead-glass calorimeter; energy ≥ 0.2 GeV; and cluster position separated from any charged-track extrapolations. In addition, the e^+e^- pairs which were consistent with γ conversion at the inner vessel of the time projection chamber (TPC) were reconstructed (1C fit) and used as γ candidates.

In order to reconstruct charm quarks, we used the decay modes $D^{*\pm} \to \pi^\pm D^0(\bar{D}^0)$, followed by $D^0(\bar{D}^0) \to K^\mp \pi^\pm X(\bar{X})$. From now on, any mention of decays includes the charge conjugation modes, for simplicity. For D^0 decays, the decay modes $D^0 \to K^-\pi^+$, $K^-\pi^+\rho^0$, $K^-\pi^+\pi^0$ ($K^{*-}\pi^+$, $K^-\rho^0$, $\bar{K}^{*0}\pi^0$), and $K^-\pi^+\pi^0\pi^0$ were

reconstructed by using kinematical constraint fits [(1–3)C]. The cuts on χ^2_{fit} were required to be greater than the 5% confidence level (C.L.). These decay modes were selected because they have relatively high acceptances, considering the branching fractions and detector acceptances. For more-than-two-body decay modes, we applied a dE/dx cut in selecting K^-; for a two-body decay, a sufficient signal-to-noise ratio was obtained without this cut. The cuts on the vector meson masses were carried out according to the detector resolution and their intrinsic decay widths. In the case of vector-plus-pseudoscalar decay, we applied a cut on the angle of the decay product of the vector meson (θ_{VP}) in its center-of-mass frame with respect to the vector meson line of flight, i.e., $|\cos\theta_{VP}| > 0.5$.

The D^{*+}'s were reconstructed with those D^0 candidates mentioned above while combining π^+'s (soft pions
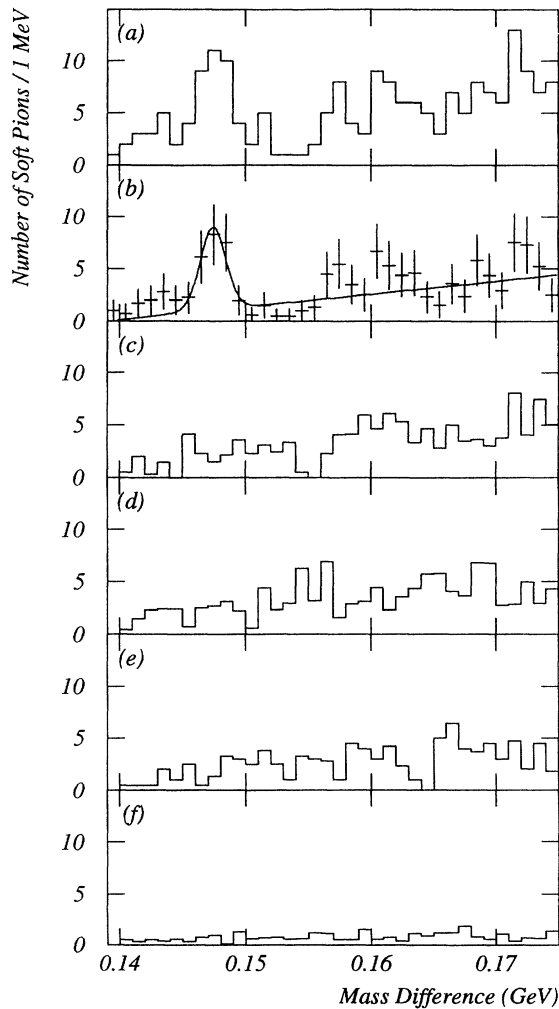

FIG. 1. Mass-difference $[dM = M(D^0\pi^\pm) - M(D^0)]$ distributions: (a) dM distribution without the weighting; (b) after the weighting. The curve is obtained from a best-fit function described in the text. (c) dM distribution for wrong-sign soft pion, (d) that for wrong-sign kaon, (e) that for wrong-sign soft pion and wrong-sign kaon, and (f) background estimation from $e^+e^- \rightarrow \gamma \rightarrow q\bar{q}$ processes.

from hereafter) with momenta less than 0.65 GeV. The energy fraction, $z = E(D^{*+})/E_{\text{beam}}$, was required to be between 0.1 and 0.25. We then calculated the mass differences, i.e., $dM = M(\pi^+D^0) - M(D^0)$. The dM distribution is plotted in Fig. 1(a).

There were multi-D^0 candidates for one soft pion which gave similar dM's. These occurred when one of the lowest momentum particles of the D^0 decay was misidentified [12]. In these cases, each entry gave a similar dM value. The differences of dM values for pairs sharing the same soft pions in the same events were plotted in Fig. 2.

The peak around zero caused an overestimate of the statistical significance of the signal. In order to address this, we carried out a weighting method, i.e., when there was more than one D^0 candidate for a given soft pion, each entry in the dM histogram was weighted by the reciprocal of the number of candidates. By this procedure, we could avoid any overestimation of the statistical significance of the peak entry. This was checked using a Monte Carlo simulation. The resulting dM distribution is shown in Fig. 1(b). The mean visible energy at the rest frame (W_{vis}) for the events containing the $D^{*\pm}$ candidates were 5.3 GeV. In order to check the peak around the $D^{*\pm}$ region, we carried out the wrong-sign combination such as $D^0\pi^-$ and etc. The results are plotted in Figs. 1(c), 1(d), and 1(e). There were no peak structures at all. The excess below the $D^{*\pm}$ peak was explained by the energy loss at support structures of the inner field cage and the central membrane of the time-projection chamber (TPC), which were distributed inhomogeneously, whereas the corrections for them were made only in average. Figure 3 shows the mass differences of two cases: (a) when the soft pion passed near these supports, and (b) when it passed far away from them.

This happened because the soft pions in the two-photon events had extremely low momenta. We counted the entries of the higher dM peak as the $D^{*\pm}$ yield in the experiment, and in the Monte Carlo simulation we corrected the peak entries about -15%, considering the
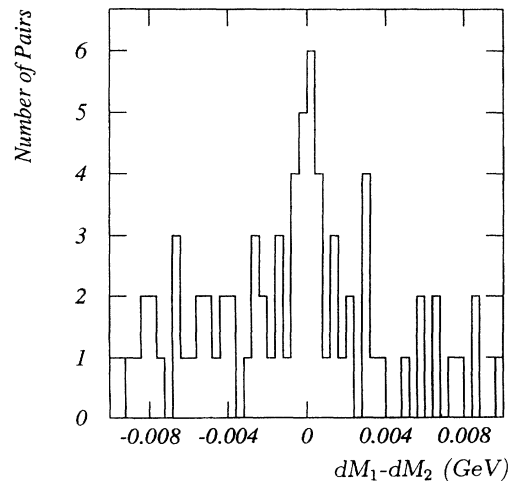

FIG. 2. Differences of dM values for pairs sharing the same soft pions in the same events.
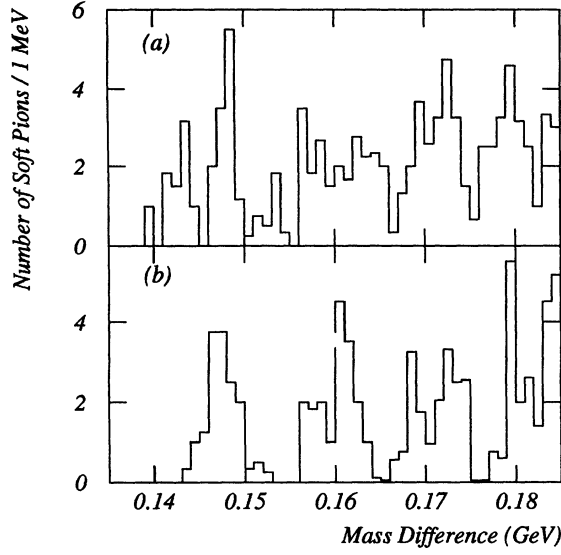
FIG. 3. Mass differences for two cases: (a) when the soft pion passed near the TPC support structures, and (b) when it passed far away from them.

amount of the materials and their solid angle from the interaction point. The error of this correction was considered to be 5% which was estimated from the e^+e^- conversion pair yield in the two-photon sample. Concerning the higher dM fluctuation, we have no explanations other than statistical fluctuations. The fitting function was the sum of a Gaussian and the following function:

$$a(dM - M(\pi^\pm))^b(1 - dM/c)^n,$$

where a, b, and c are free parameters and n is an average multiplicity of the event sample. The obtained $D^{*\pm}$ yield was 20.0 ± 5.0, where the χ^2 of the fit was 31 with $N_{df}=35$. The peak position and its width obtained by this fitting were 147.4 ± 0.2 and 0.8 ± 0.2 MeV, where the detector simulation predicted 145.4 and 1.6 MeV, respectively. We considered that the shift of the peak position was caused by the inhomogeneous material distribution described above, whereas the energy-loss correction was carried out assuming uniform material. The shift of the mass-difference peak quantitatively agreed with the expectation. The resolution difference was due to the overestimation of the material in front of the TPC in the simulation in the most probable energy-loss case. 85% of the soft pions were considered to pass away from the support structures of the TPC. We tried χ^2 and likelihood fitting and also tried polynomial background functions. The differences in the total $D^{*\pm}$ yields were within 10%. Thus we concluded that the systematic error of the fitting procedure was 10%. The yields for the four decay modes described before were 9.5 ± 3.3, 4.8 ± 2.3, 4.8 ± 2.2, and 0.9 ± 0.9, respectively.

The background from $e^+e^- \rightarrow \gamma \rightarrow q\bar{q}(\gamma)$ distributed smoothly in this dM plot [height was about 1 count per bin as shown in Fig. 1(f)]. No peak structures were obtained by the Monte Carlo simulation. We also checked the event vertex distribution in order to determine the

contamination of the beam-gas background. There was a clear peak at the interaction point with no tails.

In order to compare the experimental data with the theoretical prediction, we chose $d\sigma(D^{*\pm})/dP_T$, instead of the total cross section, as had been reported [8–10], since the accepted $D^{*\pm}$ events were limited to the high-P_T region, due to the detector acceptance. We were sensitive to those $D^{*\pm}$'s with transverse momenta (P_T) between 1.6 and 6.6 GeV. The lower limit was due to the detector acceptance and the higher due to statistics. An acceptance correction was carried out by using a lowest-order (Born-approximation) direct-process Monte Carlo simulation, in which an equivalent photon approximation was used. The $P_T(D^{*\pm})$ smearing by the P_T of the initial photons was checked by a full calculation of the $e^+e^- \rightarrow e^+e^-\gamma\gamma \rightarrow e^+e^-c\bar{c}$ process, and was concluded to be small. The hadronization was taken care of by the LUND 6.3 Monte Carlo simulation [13,14]. We did not use a parton shower option in the LUND Monte Carlo simulation, since the choice of Q^2 of the event was not well defined. The fragmentation parameters in the calculation have been tuned to reproduce the general properties of single-photon exchange processes. The systematic ambiguity for the $D^{*\pm}$ inclusive spectrum was considered to be at most 10% because the fragmentation of the $D^{*\pm}$ was measured well at various $\sqrt{s}$ and the symmetric LUND fragmentation function reproduces it very well. The systematic uncertainty of the cross section is mostly due to the fitting procedure, fragmentation scheme (described so far), the branching ratios of D^0 (Ref. [15]) and D^{*+} (Ref. [16]), the ambiguities in the detector acceptance, and the calibrations. It was estimated to be 15%. The resulting differential cross sections are 57 ± 24, 9.5 ± 5.1, 6.3 ± 3.2, and 2.0 ± 1.8 pb/GeV (systematic errors included) for P_T regions 1.6–2.6, 2.6–3.6, 3.6–4.6, and 4.6–6.6 GeV, respectively, and are plotted in Fig. 4, together with the theoretical predictions.

The raw entries at P_T binnings were 7.2 ± 2.9, 6.4 ± 3.3, 4.0 ± 2.0, and 2.4 ± 2.1, respectively, where the errors are statistical only.

Theoretical predictions for both direct and resolved photon processes were compared with this measurement as follows. In order to estimate $\sigma(D^{*\pm})$ from the theoretical calculation of $\sigma_{c\bar{c}}$, we assumed $P_{c\rightarrow D^{*\pm}}B(D^{*+} \rightarrow \pi^+D^0) = 0.185 \pm 0.024$ at $\sqrt{s} = 90$ GeV in Ref. [17]. This value is consistent with that obtained at $\sqrt{s} = 10$ GeV [18]. The events were generated by the lowest-order calculations. The relative acceptance for the process of the resolved photon to that of the direct process was obtained to be 0.76 ± 0.25 due to the event selection, where the error was especially due to the gluon density function dependence, although this ambiguity is small compared with the total contribution including the direct process. Since we did not measure the energy flow in the low-angle region, spectator jets were not detected. This lower acceptance was especially due to the lower visible energy cut of 4 GeV. The vertical scale for the cross sections of the resolved photon process shown in Fig. 4 was normalized by this factor.

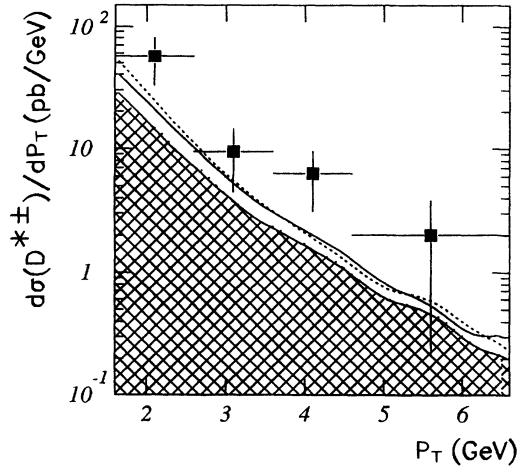Corrections of order α_s were carried out according to the procedure in Ref. [19]. Since string fragmentation

FIG. 4. $d\sigma(e^+e^- \to e^+e^-D^{*\pm}X)/dP_T$ versus P_T. The data points with error bars are the experimental data and the curves were obtained by Monte Carlo simulations while assuming various processes. The hatched area is a prediction based on the direct process, the solid curve is based on a combination of direct and resolved photon processes by the GRV parametrization, the dotted one is based on the LAC1 parametrization. The vertical scales for the resolved photon process were normalized by the relative acceptance to the direct process, because of the acceptance difference described in the text.

includes a parton-shower-like effect, the next-to-leading-order correction in the P_T spectrum is doubly counted. We used instead the P_T-independent correction to the direct process. The cross section of the direct process is increased by a factor of 1.31 uniformly, and that of the resolved photon process is corrected by a P_T-dependent function, due to the presence of the process $\gamma q \to c\bar{c}q$ (a part of this is absorbed in the gluon density function in the resolved photon). The P_T-dependent factors were obtained in the following way: At first we derived the P_T-dependent ratios between the higher and the lowest order calculations for the direct and resolved photon processes; we then calculated the factors between those of the direct and resolved photon process; and those factors were normalized to fit to the total cross section of the higher order calculations for the resolved photon process. The resultant P_T-dependent correction was written as

$$0.50P_T^c + 0.54,$$

where P_T^c is the P_T of a charm quark. The charm quark mass (m_c) and the renormalization scale (μ) were assumed to be $m_c=1.6$ GeV and $\mu = \sqrt{2}m_c$, respectively. The curves in Fig. 4 represent these predictions. The parametrization dependence for the resolved photon process appears in the lowest P_T binning. Although our data favor the Gluck-Reya-Vogt (GRV) [5] or Levy-

Abramowicz-Charchula set 1 (LAC1) [4] parametrizations, none of them explain the high P_T excess ($+1.5\sigma$ at $P_T > 2.6$ GeV).

There are ambiguities in the above-mentioned theoretical predictions, which depend on m_c and μ. We changed m_c from 1.3 to 1.8 GeV and μ from $m_c/2$ to $2m_c$. The lower m_c and μ give a higher cross section which has a P_T dependence. The lowest P_T region may be explained by such ambiguities as mentioned above, and the threshold enhancement of $c\bar{c}$ production. We thus concentrate on the higher-P_T regions, i.e., $P_T > 2.6$ GeV. The case for $m_c = 1.3$ GeV and $\mu = m_c/2$ gives the highest one, i.e., $+0.54$ pb ($+6\%$) higher than the nominal value. The experiment gives $\sigma(2.6 < P_T < 6.6$ GeV)$= 19.8\pm7.0$ pb, where the GRV parametrization predicts 9.0 ± 0.5 pb. Then the difference is 10.8 ± 7.5 pb.

In addition, if gluons inside the photon have P_T's of 0.4 GeV in average, the P_T's of $c\bar{c}$'s are shifted. This may increase the resolved photon cross section by about a factor of 2, because the spectrum of this process is proportional to an exponential function. Therefore, the ~ 2–3 pb increase may be expected for this reason (no increase in the direct process). In this case, our results become consistent with the expectation within the 1σ level.

Such event shapes as missing P_T and thrust distributions were checked. These shapes are consistent with the prediction of the lowest-order direct and resolved photon processes, except for the overall normalization factor.

In a part of the data set (integrated luminosity of 90 pb^{-1}), there were forward calorimeters (FCL) made of bismuth germanate crystal (BGO) which covered the polar angle region between 3.2 and 13.6 degrees [20]. We analyzed tagged events by the FCL with the same analysis. We observed the total $D^{*\pm}$ yield to be 3.5 ± 3.6, where the lowest-order direct process predicts 1.0 ± 0.4 events. We therefore need more statistics in order to observe tags from electrons and positrons as well as spectator jets.

In conclusion, we measured the inclusive $D^{*\pm}$ production cross section in two-photon collision events at the TRISTAN e^+e^- collider. The mean $\sqrt{s}$ was 57.16 GeV and the integrated luminosity was 150 pb^{-1}. We observed $(20 \pm 5)D^{*\pm}$ in our data sample. The production cross section in the high-P_T region was $\sigma_{D^{*\pm}}(2.6 < P_T < 6.6$ GeV)$=19.8\pm7.0$ pb. Comparisons with the theoretical prediction of the direct process and the resolved photon process were carried out.

[1] See, e.g., S. J. Brodsky, T. Kinoshita, and H. Terazawa, Phys. Rev. D **4**, 1532 (1971).

[2] D. W. Duke and J. F. Owens, Phys. Rev. D **26**, 1600 (1982).

[3] M. Drees and K. Grassie, Z. Phys. C **28**, 451 (1985).

[4] H. Abramowicz, K. Charchula, and A. Levy, Phys. Lett. B **269**, 458 (1991).

[5] M. Glück, E. Reya, and A. Vogt, Phys. Rev. D **46**, 1973 (1992).

[6] Ch. Berger et al., Z. Phys. C **33**, 351 (1987); H. -J. Behrend et al., Z. Phys. **C51**, 365 (1991); H. Aihara et al., Phys. Rev. D **41**, 2667 (1990); R. Tanaka et al., Phys. Lett. B **277**, 215 (1992).

[7] M. Drees, M. Krämer, J. Zunft, and P. M. Zerwas, Phys. Lett. B **306**, 371 (1993).

[8] W. Bartel et al., Phys. Lett. B **184**, 288 (1987).

[9] W. Braunschweig et al., Z. Phys. C **47**, 499 (1990).

[10] M. Alston-Garnjost et al., Phys. Lett. B **252**, 499 (1990).

[11] R. Enomoto et al., Nucl. Instrum. Methods Phys Res. Sect. A **269**, 507 (1988); A. Imanishi et al., ibid. **269**, 513 (1988); T. Kamae et al., ibid. **252**, 423 (1986); A. Yamamoto et al., Jpn. J. Appl. Phys. Lett. **25**, L440 (1986); S. Kawabata et al., Nucl. Instrum. Methods Phys.

Res. Sect. A **270**, 11 (1988); J. Fujimoto et al., ibid. **256**, 449 (1987); S. Noguchi et al., ibid. **271**, 464 (1988).

[12] H. Aihara et al., Phys. Rev. Lett. **53**, 2465 (1984).

[13] T. Sjöstrand, Comput. Phys. Commun. **39**, 347 (1986); T. Sjöstrand and M. Bengtsson, Comput. Phys. Commun. **43**, 367 (1987). The symmetric LUND fragmentation function with $\sigma_q = 0.42$, $a=0.9$, and $b=0.61$ without parton shower option was used. These parameters were fitted with single γ annihilation hadronic events, as described in I. Adachi et al., Phys. Lett. B **227**, 495 (1989). These parametrizations also reproduce the charm meson fragmentation function at lower energies.

[14] H. Hayashii et al., Phys. Lett. B **314**, 149 (1993).

[15] Particle Data Group, K. Hikasa et al., Phys. Rev. D **45**, S1 (1992).

[16] F. Butler et al., Phys. Rev. Lett. **69**, 2041 (1992).

[17] D. Decamp et al., Phys. Lett. B **266**, 218 (1991).

[18] D. Bortoletto et al., Phys. Rev. D **37**, 1719 (1988); **39**, 1471 (1989).

[19] J. Smith and W. van Neerven, Nucl. Phys. **B274**, 36 (1992).

[20] H. Hayashii et al., Nucl. Instrum. Methods Phys. Res. Sect. A **316**, 202 (1992).